Front. Struct. Civ. Eng. 2014, 8(1): 46–56
DOI 10.1007/s11709-014-0237-y

RESEARCH ARTICLE

An experimental study on the flexural behavior of heavily steel reinforced beams with high-strength concrete

Yasser SHARIFI[a*], Ali Akbar MAGHSOUDI[b]

[a] *Department of Civil Engineering, Vali-e-Asr University of Rafsanjan, Rafsanjan, Iran*

[b] *Department of Civil Engineering, Shahid Bahonar University of Kerman, Kerman, Iran*

[*] *Corresponding author. E-mail: y.sharifi@vru.ac.ir*

ABSTRACT In recent years, an emerging technology termed high-strength concrete (HSC) has become popular in construction industry. Present study describes an experimental research on the behavior of high-strength concrete beams in ultimate and service state. Six simply supported beams were tested, by applying comprising two symmetric concentrated loads. Tests are reported in this study on the flexural behavior of high-strength reinforced concrete (HSRC) beams made with coarse and fine aggregate together with Microsilica. Test parameter considered includes effect of being compressive reinforcement. Based on the obtained results, the behavior of such members is more deeply reviewed. Also a comparison between theoretical and experimental results is reported here. The beams were made from concrete having compressive strength of 66.81–77.72 N/mm^2 and percentage reinforcement ratio (ρ/ρ_b) in the range of 0.56% – 1.20%. The ultimate moment for the tested beams was found to be in a good agreement with that of the predicted ultimate moment based on ACI 318-11, ACI 363 and CSA-04 provisions. The predicted deflection based classical formulation based on code provisions for serviceability requirements is found to underestimate the maximum deflection of HSC reinforced beams at service load.

KEYWORDS high-strength concrete (HSC) members, flexural behavior, reinforced concrete, experimental results, ultimate moment

1 Introduction

Research work conducted in recent years has improved our knowledge of the potential of mixtures of chemicals and minerals. This knowledge has made it possible to manufacture concretes with high mechanical properties, with successive improvements with regard to workability and durability. It has been found that high-strength reinforced concrete is particularly competitive in many structures, such as long span bridges where, strength, durability and service behavior are particularly important. Given its considerable advantages over normal-strength concrete, the use of high-strength concrete has increased rapidly in the last ten years and it is inevitable that it will come to be used in other areas of construction in the near future. Advances in concrete technology in many countries have now made practical to use concrete with strengths up to 90 MPa. It is widely known this concrete becomes less deformable and more brittle when it's compressive strength increases especially when it is heavily reinforced [1–4]. In this study heavily steel beam is defined as the beam that its reinforcement ratio (ρ/ρ_b) is upper than 0.5.

High strength concrete (HSC) provides a better solution for reduce sizes and weights of concrete structural element [5–8] particularly for long-span beams. This reduction in cross sectional members which reflects on the moment of inertia, I, of the members necessitates the investigation of the corresponding deflection under the service load. The moment of inertia of a reinforced concrete beam depends on the degree of cracking load in the member. For loads below the cracking load, computation of deflection may be based on the gross moment of inertia, I_g, of the concrete section ignoring the reinforcement. However, as the load increases above the cracking load the member cracks at discrete intervals along the span. The neutral axis fluctuates between cracks, causing a variation of curvature

Article history: Received Sept. 21, 2013; Accepted Nov. 29, 2013

along the member length and reducing the flexural rigidity of the section.

Despite a large number of investigations [1–23] carried out in the past on flexural behavior of high-strength concrete (HSC) beams, controversy still remains with regard to some vital design issues. One such issue is the serviceability consideration specially deflection. Flexural members tested by several investigator demonstrated significantly larger deflections at service load that what would be predicted by following the ACI 318-11 code [5] recommend. Even the assumption of cracked moment of inertia as the effective value and use of the representative expressions for the effective moment of inertia for span beam length as reported by ACI 318-11 committee [24] has failed to bring the predictions on the conservative side. Therefore, explanations must be sought through further investigations. Ashour et al. [10] believe that the utilization of HSC impacts the parameters involved in the deflection calculations. This includes concrete modules of elasticity and cracked moment of inertia. He modified the previously proposed formula for the effective moment of inertia. Another important design issue is the modules of rupture cracking moment of a HSC reinforced. In the present paper, HSC reinforced beams sustain lower load at flexural cracking in compare with the ACI 318-11 and CSA-04 codes provisions estimation.

The majority of recent studies have provided information on the under-reinforced sections, therefore the lack of data on over-reinforced sections made the authors to investigate the behavior of heavily steel reinforced HSC beams. It should be reminded that the heavily steel reinforced concrete sections are not suitable for employing in seismic zones; nevertheless it has been decided to demonstrate the behavior of these members to provide the informative conclusions on ultimate and serviceability response of such section when employing HSC. The objective of this research is to investigate the effect of compressive reinforcement on behavior of heavily steel reinforced HSC beams under bending. In this paper the ultimate and serviceability requirement of deflection of such members are described and the experimental results are compared with the theoretical calculations that are predicted based on the ACI 318-11 [5] and CSA-04 [25] codes provisions.

2 Experimental program

2.1 Test specimens

Six simply supported reinforced concrete beams were tested under two point loading with a constant moment region [26,27]. Table 1 presents the detailed testing program. Three beams were singly reinforced and the other three were doubly reinforced. Shear reinforcements were provided along the beam length except in the constant moment region. The variables were the compressive reinforcement ratio ρ and ρ'.

Each beam was designated using letters and numbers. The letters "B" refers to the singly reinforced beams and the letter "BC" refers to corresponding beams with compressive reinforcement. The numbers 6, 7 and 8 followed by the letter refers to the percentage of tension reinforcement ratios (ρ) 4.81%, 5.38% and 6.80% respectively. The compression reinforcement ratios (ρ') have been choosen half of the tension reinforcement for all doubly reinforced beams. All the beams were cast in steel molds and the companion concrete specimens were cast in standard steel molds. For each mix, three numbers of 150 mm × 300 mm cylinders for compressive strength were cast and compaction was done using Φ25 mm needle vibrator for beams. The beams and the companion concrete specimens were demolded after 24 h and were cured with wet hessian (spraying the water twice a day, similar to site curing) for 6 days. After that, the specimens were air-cured with relative humidity of 65% – 80% and ambient temperature 28±3°C until the age of testing.

As it is evident from Table 1, for the single reinforcement beams (B6, B7 and B8) the longitudinal reinforcement is more than the maximum allowable longitudinal reinforcement based on the provision of ACI 318-11. It should be stated that the longitudinal reinforcement of beams is less than the needed tensile reinforcement for balance state, therefore it has been named heavily steel reinforcement. In other words, heavily steel reinforcement is a transient phase between under-reinforcement and over-reinforcement beam's conditions. In author opinion there was no clear recommendations on the behavior these types of beams as made of HSC. Moreover, it has been tried to consider the effect of compressive reinforcement as much

Table 1 Testing program detail of tested beam [26,27]

beam No.	f_c' /MPa	d/mm	d'/mm	A_s	A_s'	ρ'/ρ	ρ/ρ_b	ρ_{max}/ρ_b
BC6	73.65	256	40	4Φ28	2Φ28	0.5	0.56	0.707
B6	71.00	256	–	4Φ28	–	0.0	0.79	0.707
BC7	66.81	266	40	4Φ28 + 2Φ16	3Φ22 + 2Φ14	0.5	0.72	0.707
B7	70.50	266	–	4Φ28 + 2Φ16	–	0.0	0.91	0.707
BC8	77.72	258	42	2Φ28 + 6Φ22	2Φ28 + 2Φ14 + 1Φ16	0.5	0.71	0.707
B8	71.80	258	–	2Φ28 + 6Φ22	–	0.0	1.20	0.707

as half percent of tensile reinforcement on the behavior of HSC heavily steel reinforcement beams. As it can be seen from Table 1, by adding half of tensile reinforcement as compression reinforcement the longitudinal tensile to balance reinforcement ratio decreased to maximum allowable longitudinal reinforcement, approximately. Therefore, it has been decided to investigate the response of doubly reinforcement beams and compare with those initial situation (singly reinforcement).

2.2 Materials

Locally available deformed bars were used as flexural reinforcement. The average yield strength of the longitudinal reinforcement was found to be approximately 390 MPa from the tension tests performed in the laboratory. The detailed mix proportions are shown in Table 2. All beams and control specimens were cast and cured under similar conditions. A sufficient mixing time was allowed to produce a uniform and homogenous concrete. The concrete strength of each beam was measured by three 150 mm × 300 mm concrete cylinder specimens made at time of casting and were kept with the beams during curing. The Portland cement type-II, the coarse and fine aggregates desert sand with modulus of 3.1, and coarse aggregate (crushed basalt) of 10 mm maximum size were used. Light gray densified micro silica (20% by weight of cement) with a specific gravity of 2.2, a bulk density of 6.0 kN/m^3, and a specific surface of 2.3 m^2/g was used for the HSC mix. A super plasticizer was used and enough mixing time was allowed to produce uniform mixing of concrete without any segregation.

2.3 Test procedure

The test beams were simply supported and subjected to two-point loads, as shown in Fig. 1. The beam deflections were measured at four section using transducers. Strains in the tension and compression steel were measured by electrical strain gauges. Compressive strains at the surface of the concrete at different sections were measured with electrical and mechanical (demec points) strain gauges. The beams were instrumented with linear voltage displacement transducers (LVDT) at mid span to monitor deflection. Mechanical strain gauges (demec) were used to measure the concrete strain at the surface in the pure bending region. Steel strains were measured using PL-30-11 gauges. The steel strain gauges were covered with silicone gel to prevent the accidental damage during casting. The crack width measurements were made using a hand-held microscope of X40 magnification with least count of 0.02 mm. All the strains and deformation readings were recorded automatically using data logger during the test. Arrangement of each set up for test takes at least one day, therefore it has been tested the specimens in six days consecutively. As concrete compressive strengths were evaluated based on 28 days, it tried to test all beams from days 28 to 33. As obtaining the structural behavior of specimens in critical points (crack, yield and ultimate) are important and sensitive, it has been also tried to examine test specimens with closer loading rate in these points.

3 Experimental results and discussion

All of the beams have been designed to fail in flexure. Figure 2 show the crack propagation and collapse of beams under loading. All beams exhibited vertical flexural cracks in the constant moment region before failure of the beams due to crushing of compressive concrete. The experimental load-strain curves in midspan for both tensile and compression reinforcements have been plotted in Fig. 3. It should be noted that the strain gauge which has been mounted on the tensile reinforcement of BC7 disconnected before the ultimate load. This trend can be found from Fig. 3(a), where the tensile strain of specimen BC7 will not reach its ultimate strain.

3.1 Ultimate neutral axis depth

Experimental data which were obtained from strain gauges in compression concrete and steel reinforcement have been employed to account the neutral axis (NA) depth (X) based on the Fig. 4. The variation of the experimental neutral axis, NA, depth versus load for single and duble reinforced beams have been shown in Fig. 5. Some fluctuations of the NA depths (especially for singly reinforcement beams) took place at loading due to the sensivity of the strain gauges reading especially before cracking. The Figures show that the depth of NA does not vary between cracking and yielding levels. The results also show that, by adding ρ' to the singly reinforced beams the depth of NA at yield and ultimate state has been decreased (Fig. 5). It is clear that using compressive reinforcement give more ductlity compare with the singly reinforced beams, this can be found from Fig. 5, where the NA depths of doubly reinforced specimens (BC) are less than of corresponding those without compressive reinforcement (B).

The theoretical $X_{u(th\text{-}ACI)}/d$ and $X_{u(th\text{-}CSA)}/d$ (ultimate neutral axis-to-depth ratio) can be calculated based on the

Table 2 Concrete mix proportion

cement/(kg·m^{-3})	microsilica/(kg·m^{-3})	coarse agg./(kg·m^{-3})	fine agg./(kg/m^3)	super-plasticizer/(kg·m^{-3})	W/C ratio
649	55	723	646	11	0.32

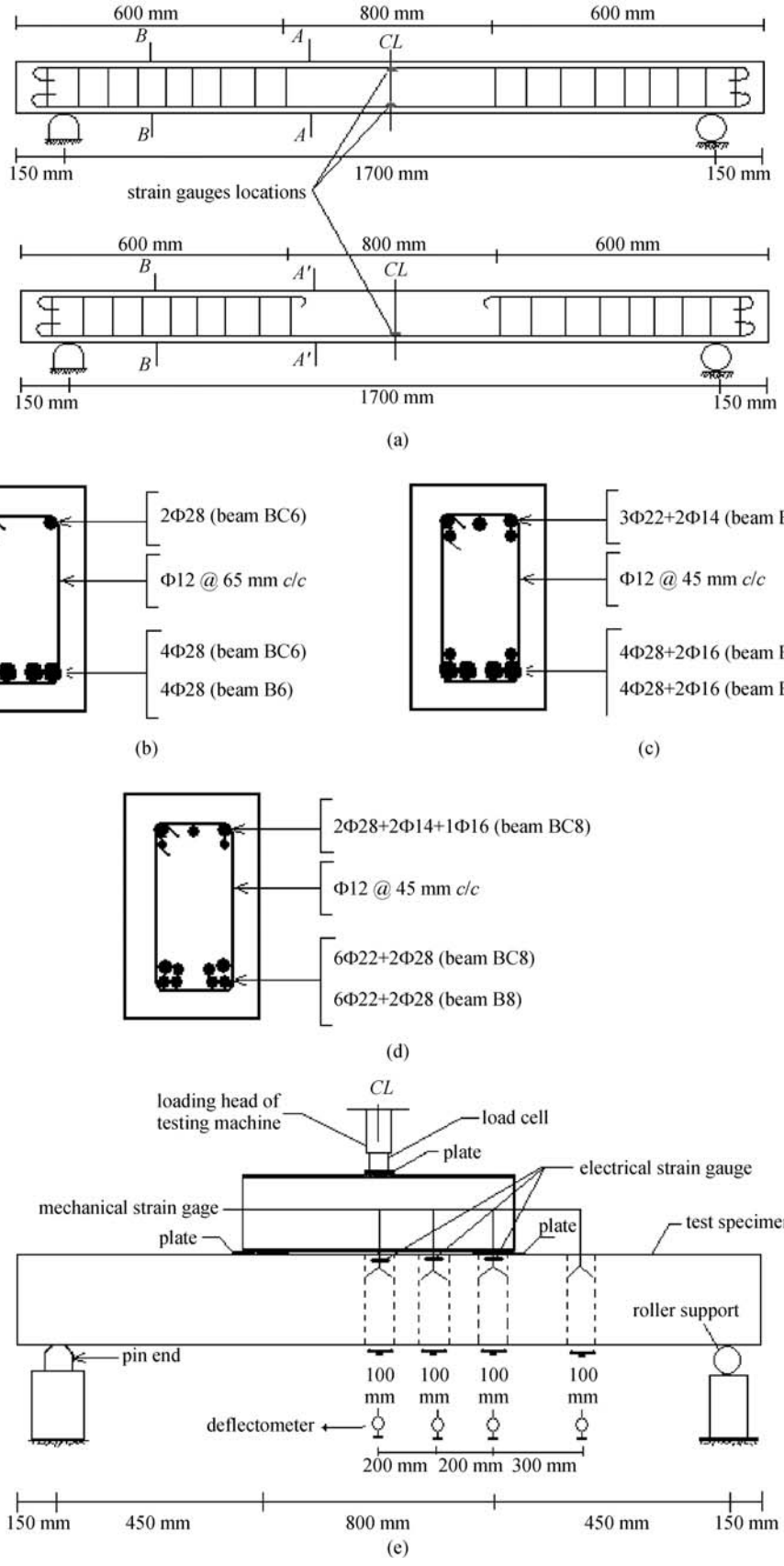

Fig. 1 (a) Details of tested beam; (b) details of sections for beams B6 and BC6; (c) details of sections for beams B7 and BC7; (d) details of sections for beams B8 and BC8; (e) testing arrangement

(a)

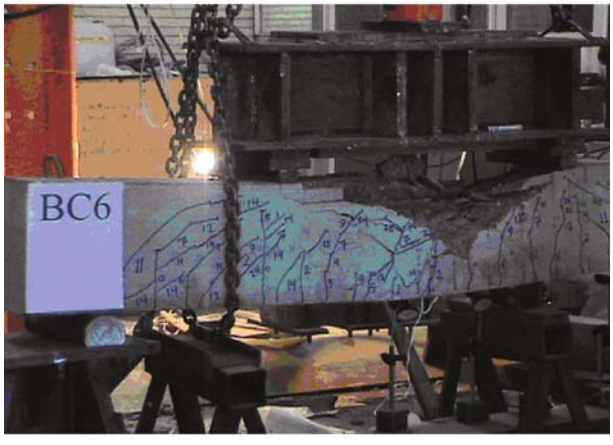

(b)

(c)

Fig. 2 (a) Crack propagation of beam B6 under load; (b) collapse of beam BC6 under load; (c) crack propagation of beam BC7 under Load

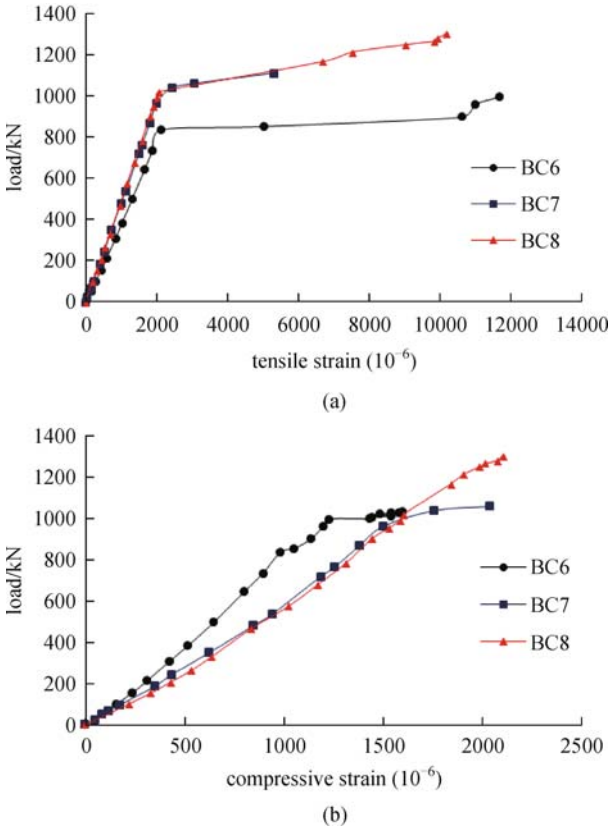

Fig. 3 (a) Load-tensile strain of beams BC6-BC8 in midspan; (b) load-compressive strain of beams BC6-BC8 in midspan

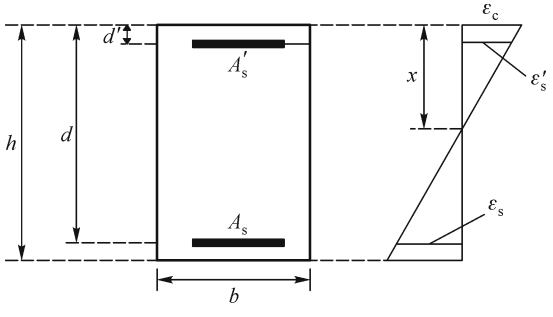

Fig. 4 Beam cross section and strain distribution

rectangular stress block given in ACI 318-11 and CSA-04 and utilizing the Eqs. (1) – (13) that can be found in any fundamental concrete books (e.g., Ref. [28]). The experimental and theoretical results for ultimate neutral axis-to-depth ratio have been presented in Table 3.

It can be found from test results that the NA depth increases as tensile reinforcement ratio increases. This trend was also expected, because increasing tension reinforcement causes more fragility and hence greater NA depth. Therefore, a lower reinforcement ratio ensures that the depth of NA is lower, hence leading to ductile failure. By adding the compression reinforcement to the beam section the ultimate NA depth was decreased. The theoretical values based on the code provisions, are greater than the experimental neutral axis depth in ultimate state. This can be attributed to the strain hardening phenomenon, because in the classical methods based codes formulations (Eqs. (1) – (13)) the strain hardening that give more tension reinforcement stress is not considered and the maximum stress has been restricted to f_y. The other reason is the coefficients of the stress block (α, β_1) which maybe needs

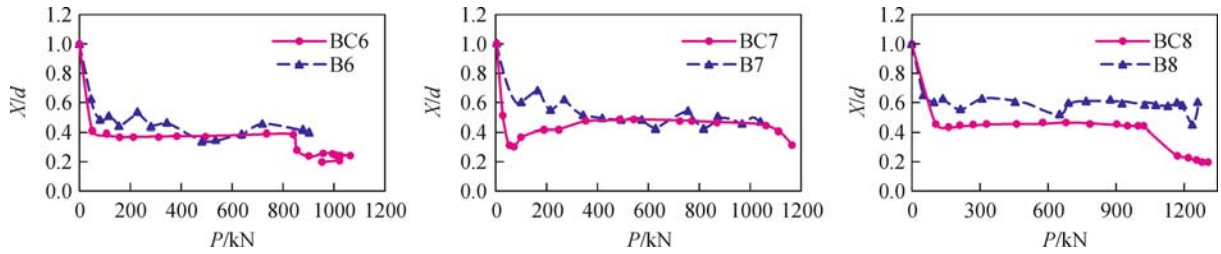

Fig. 5 Behavior of neutral axis depth under load

to be more reformed compare with the given coefficients based ACI 318-11 and CSA-04 codes suggestions values.

3.2 Ultimate moment

The theoretical ultimate moments have been calculated by using the fundamental equations based on ACI 318-11 and CSA-04 codes suggested values, named $M_{u(th\text{-}ACI)}$ and $M_{u(th\text{-}CSA)}$, respectively. The experimental yielding moment, $M_{y(exp)}$, corresponds to the moment at the beginning of the yielding flat plateau in the moment–curvature curve which have been predicted precisely from the data of mounted strain gauges on the tension reinforcements in this paper, and experimental ultimate moment $M_{u(exp)}$, is the moment obtained from the ultimate load reached during testing are also estimated based on the experimental results. The predicted design moments ($M_{u(th\text{-}ACI)}$ and $M_{u(th\text{-}CSA)}$) and the experimental yield ($M_{y(exp)}$) and ultimate moment ($M_{u(exp)}$) are shown in Table 4. A comparison between two codes (ACI 318-11 and CSA-04) for the theoretical values are also shown in this Table, it is evident that for all the tested beams, the ACI 318-11 values are higher than the CSA-04 values.

The average ratios of experimental strength to predicted strength were 1.034 and 1.043 for ACI 318-11 and CSA-04 code provisions, respectively. The strength of HSC heavily steel reinforced beam were quite close to that of the predicted by codes. In the previous researches that were investigated approximately on the under-reinforced beams consisting high-strength concrete, the experimental strength were greater than the theoretical that predicted based on the codes method. Rashid and Mansur [24] tested 16 high-strength concrete beams and the results show that the ACI 318-11 code provisions give a reasonable estimate for the ultimate moment capacity of the test beams with a mean of 1.09 for the ratio of experimental-to-predicted values and also he collected the experimental ultimate moments of a large number (93 beams) of HSC beams from the literatures and compared with the respective calculated values and once again, good agreement was found between the measured and estimated values and for a total of 93 beams, the ratio $M_{u(exp)}/M_{u(th\text{-}ACI)}$ has an average of 1.12.

3.3 Ultimate curvature and deflection

The experimental midspan ultimate curvature which is concluded from Fig. 4 and also the theoretical ultimate curvatures which have been evaluated in two current codes provisions [5,25], are presented in Table 5. The experimental ultimate deflections $M_{u(exp)}$, compressive concrete strain at the top surface, $\varepsilon_{cu(exp)}$, and tension steel strain, $\varepsilon_{su(exp)}$ at midspan for all beams are presented in Table 5.

The ultimate concrete strain is assumed as 0.003 and 0.0035 for two codes, ACI 318-11 and CSA-04 provisions, respectively and these are employed to estimate the theoretical ultimate curvatures. It has been shown by many researchers that the ultimate concrete strain of HSC varies from 0.002 to 0.004 or even more especially when the concrete made from reactive aggregates. Therefore it is necessary to revise rectangular stress-strain parameters to integrate the concrete strength as a function to evaluate

Table 3 Experimental neutral axis depth measured at cracking, yield and ultimate loads

beam no.	$X_{u(exp)}/d$	$X_{u(th\text{-}ACI)}/d$	$X_{u(th\text{-}CSA)}/d$	$\frac{X_{u(exp)}/d}{X_{u(th\text{-}ACI)}/d}$	$\frac{X_{u(exp)}/d}{X_{u(th\text{-}CSA)}/d}$
BC6	0.257	0.301	0.351	0.85	0.74
B6	0.475	0.496	0.579	0.96	0.82
BC7	0.320	0.377	0.440	0.85	0.73
B7	0.591	0.512	0.598	0.98	0.84
BC8	0.322	0.418	0.488	0.77	0.66
B8	0.594	0.625	0.729	0.95	0.82
average value				0.89	0.77

Table 4 Experimental and theoretical bending moment of tested beams

beam No.	$M_{u\ (exp)}$ /(kN·m)	$M_{y(exp)}$ /(kN·m)	$M_{u(th\text{-}ACI)}$ /(kN·m)	$M_{u(th\text{-}CSA)}$ /(kN·m)	$M_{u(exp)}/M_{y(exp)}$	$M_{u(exp)}/M_{u(th\text{-}ACI)}$	$M_{u(exp)}/M_{u(the\text{-}CSA)}$
BC6	239.75	188.16	251.09	249.55	1.274	0.955	0.961
B6	214.74	179.96	204.93	203.80	1.193	1.0478	1.0536
BC7	276.65	234.03	290.64	288.23	1.182	0.952	0.9598
B7	241.69	191.75	240.83	239.16	1.260	1.003	1.010
BC8	303.20	249.33	339.73	335.70	1.216	0.8925	0.9032
B8	281.94	238.97	252.80	250.81	1.179	1.1152	1.1241
average value					1.217	0.994	1.002

Table 5 Experimental measurements and ultimate curvature of tested beams

beam No.	$\varnothing_{u(exp)} \times 10^{-5}$ /(1/mm)	$\varnothing_{u(th\text{-}ACI)} \times 10^{-5}$ /(1/mm)	$\varnothing_{u(th\text{-}CSA)} \times 10^{-5}$ /(1/mm)	ultimate deflection, $\Delta_{u(exp)}$/mm	ultimate steel strain, $\varepsilon_{su(exp)}$	ultimate concrete strain, $\varepsilon_{cu(exp)}$
BC6	6.24	3.89	4.95	19.70	0.0125	0.0041
B6	2.55	2.36	2.94	9.70	0.0019	0.0031
BC7	5.67	2.99	3.82	25.67	0.0056[a]	0.0025[a)]
B7	2.25	2.20	2.74	12.84	0.0030	0.0030
BC8	5.07	2.78	3.45	16.73	0.0109	0.0042
B8	2.48	1.86	2.10	14.00	0.0016	0.0038

[a)] Last reading taken before the gauge is disconnected

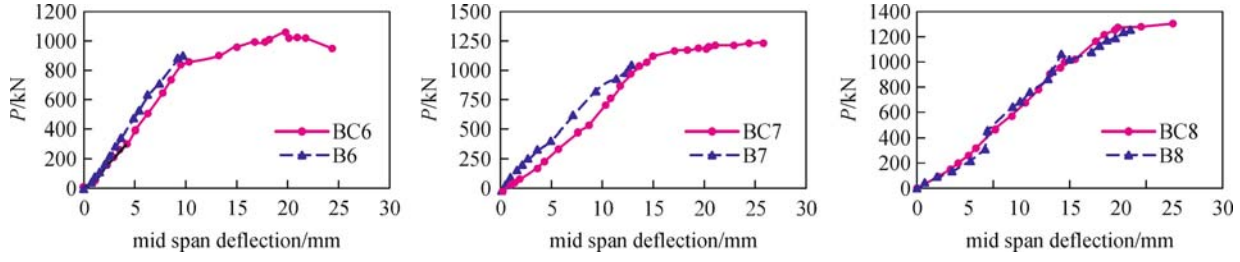

Fig. 6 Deflection beams curves of midspan load

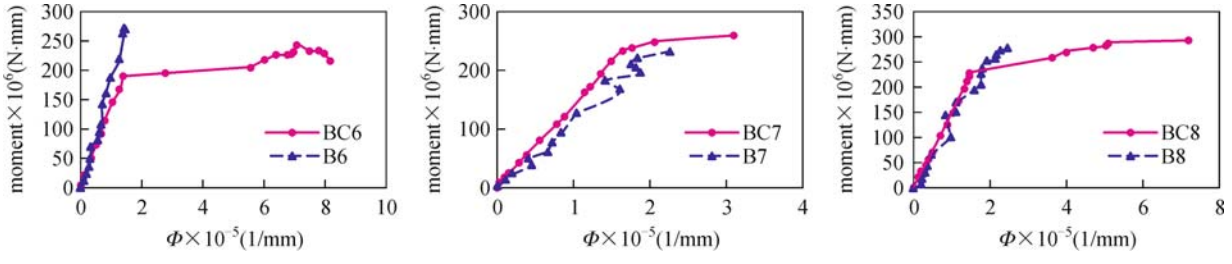

Fig. 7 Curvature beams curves of midspan moment

ultimate concrete strain. The experimental load-deflection and moment-curvature curves have been plotted in Figs. 6 and 7, respectively. Behavior and trend of the single and double reinforcement sections has been compared in these figures.

It can be found that by adding compressive reinforcement to the beam section, the curvature, deflection, compressive concrete strain and tension steel in ultimate state are increased. In other words by adding compressive reinforcement the ductility is increased. Comparison

Table 6 Experimental and theoretical cracking bending moment of tested beams

beam No.	$M_{cr(exp)}$/(kN·m)	$M_{cr(th\text{-}ACI)}$/(kN·m)	$M_{cr(th\text{-}CSA)}$/(kN·m)	$M_{cr(exp)}/M_{cr(th\text{-}ACI)}$	$M_{cr(exp)}/M_{cr(th\text{-}CSA)}$
BC6	12.05	15.89	15.38	0.7583	0.7835
B6	9.90	15.52	15.02	0.6378	0.6591
BC7	11.31	15.20	14.72	0.7441	0.7683
B7	10.79	15.47	14.96	0.6975	0.7212
BC8	11.46	16.39	15.86	0.6992	0.7225
B8	10.64	15.61	15.10	0.6816	0.7046
average value				0.7031	0.7265

between experimental and theoretical ultimate curvatures showed that for singly reinforced beams the results values are close compare to the doubly reinforced beams.

3.4 Cracking moment

The analytical evaluation of deflection depends greatly on the cracking moment of the beams. Cracking moment, M_{cr} is usually estimated using the modulus of rupture as

$$M_{cr} = \frac{f_r \cdot I_g}{y_t}, \tag{1}$$

where f_r is the modules of rupture and their different values for two codes are presented as: $f_r = 0.62\sqrt{f'_c}$ MPa (ACI 318-11) and $f_r = 0.6\lambda\sqrt{f'_c}$ (λ = 1, for concrete with ordinary special weight) MPa (CSA-04). y_t is the neutral axis depth from the bottom side of the beam and I_g is the grass moment of inertia.

The experimental cracking moment, $M_{cr(exp)}$, which correspondes to the moment at which the initial slope of the load-deflection curve deviates [10]. Here, visual inspection during the test in all loading steps employed to estimate the first flexural cracking and hence cracking moment. Experimental cracking moment, $M_{cr(exp)}$, is employed to determine the experimental cracking stress, f_r. The value of f_r is usually depends on several factors such as crack observation technique, sensitivity to residual stresses, etc. [11]. The obtained experimental cracking moment is presented in Table 6. The experimental cracking moment $M_{cr(exp)}$, are compared with the corresponding moments calculated by using two different code approaches [5,25] for the tested beams. The theoretical cracking moments which are predicted based on two code provisions are greater than experimental cracking moment. It should be noted that based on the codes provisions equations to assess the cracking stress (Eq. (1)), only compressive strength of concrete is influence, further more it cannot be accurate for reinforced concrete beams to calculate the cracking moment. Therefore maybe it is necessary to revise the modulus of rupture parameters in reinforced concrete beams consisting HSC, to integrate the other parameters as functions to evaluate cracking moment. The relationships between experimental modules of ruptures that have been estimated from test results versus corresponding compressive strengths of concrete are shown in Fig. 8. It can be found from Fig. 8 that the current experimental test results give the lower value compare to code provisions. Therefore, it needs more details experimental investigations to assess the exact modules of rupture of HSC reinforced beams.

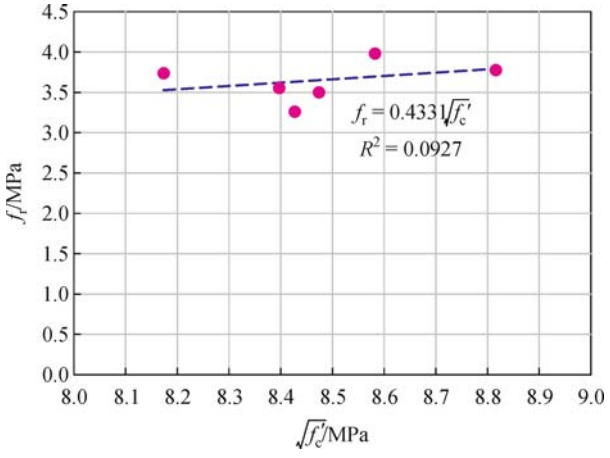

Fig. 8 Modules of rupture versus compressive strength of concrete of tested beams

3.5 Maximum deflection at service load

To investigate the service load behavior with respect to deflection, maximum (midspan) deflections, ($\delta_{ser,ACI}$) at service load (experimental ultimate load divided by a factor of 1.7) [24] are calculated for the test beams using the elastic bending theory as

$$\delta_{ser} = \frac{M_a}{24E_cI}(3L^2 - 4a^2), \tag{2}$$

where M_a is the applied maximum (mid-span) moment; L is the beam span; a is the shear span.

E_c is the modulus of elasticity of concrete and the value of moment inertia, I changes along the beam span from a maximum value of I_g for uncracked (gross) section to a

minimum value of I_{cr} for the fully cracked (transformed) section. The variation of I along the span length not only makes the deflection calculation lengthy and tedious but also, its accuracy is difficult. Hence, in a cracked member, to provide a smooth continuous transition between I_g and I_{cr}, over the entire length of a simply supported beam, ACI 318-11 recommends the use of the following expression for the calculation of the effective moment of inertia

$$I_e = I_{cr} + (I_g - I_{cr})\left(\frac{M_{cr}}{M_a}\right)^3 \leqslant I_g, \quad (3)$$

in which M_{cr} is the cracking moment of beam (as mentioned in Section 3.4) and I_g and I_{cr} are moments of inertia of gross and cracked sections, respectively.

To assess the I_{cr} traditional theoretical definition based on the cracked transformed section can be given as [29]:

(a) Singly reinforcement beams

$$\frac{bc^2}{2} + nA_s c - nA_s d = 0, \quad (4)$$

$$I_{cr} = \frac{bc^3}{3} + nA_s(d-c)^2, \quad (5)$$

where $n = \frac{E_s}{E_c}$ and $E_c = (3200\sqrt{f'_c} + 6900)\left(\frac{w_c}{2300}\right)$ (MPa) (ACI 363 [30]).

(b) Doubly reinforced beams

$$\frac{bc^2}{2} + (A_s + {}_s)nc - (A_s d + A'_s d')n = 0, \quad (6)$$

$$I_{cr} = \frac{bc^3}{3} + nA_s(d-c)^2 + (n-1)A'(c-d')^2. \quad (7)$$

Comparisons between the calculated ($\delta_{ser,ACI}$) and the corresponding experimental deflections ($\delta_{ser,exp}$) at service load, as shown in Table 7, indicate that the use of ACI 318-11 code expressions for f_r and E_c leads to highly unconservative predictions ($\delta_{ser,ACI}$). As it was expected, doubly reinforced beams sustain more deflections compare to those of single reinforced at service load. Average ratio of measured deflection to the predicted deflection based on ACI 318-11 was 2.31. The total deflections under service load for the tested beams varied from 5.45 to 10.33 mm. These measured deflections are based on short-term loading and do not allow any time dependent increase due to shrinkage and creep. This may be the reason for excessive deflection. Beside this, may be the effective moment of inertia based ACI 318-11 code do not give the appropriate value for cracked moment inertia along of HSC reinforced beams span. Following based an approach the experimental cracked moment of Inertia have been compared with the theoretical corresponding measurements.

The experimental cracked moment of inertia, $I_{cr(exp)}$, can be defined as the slope of the line connecting the origin and point of initial yielding of the tensile reinforcement in moment curvature curve [10,28,29]. This is given as

$$I_{cr(exp)} = \frac{M_y}{E_c \phi_y}, \quad (8)$$

where $\phi_y = \frac{\varepsilon_{cy} + \varepsilon_{sy}}{d} = \frac{\varepsilon_{cy}}{X_y}$, ε_{cy} = the measured compressive concrete strain in extreme fiber in section as steel reinforcement yields, ε_{sy} = the yield strain of tensile steel reinforcement, X_y = neutral axis depth at yielding state.

The difference in values of $I_{cr(exp)}$ and $I_{cr(th)}$, which has been described abovementioned, is expected due to the great variation in curvature distribution along the beam especially due to the peaks in curvature at the cracks location. The results of theoretical and experimental cracked moment of inertia are presented in Table 8. It is evident that the values of $I_{cr(exp)}$ is lower than the values of $I_{cr(th)}$.

4 Concluding remarks

The study investigated the implications of using HSC in reinforced beams. Moreover, the emphasis is on adding the compressive reinforcement to the single reinforcement members to compare behavior of such member with the beams without compressive reinforcement. The following conclusions are found based on the experimental test of heavily steel reinforced HSC beams:

Table 7 Experimental and predicted deflection at service load

beam type	$\delta_{ser,exp}$/mm	$\delta_{ser,ACI}$/mm	$\delta_{ser,exp}/\delta_{ser,ACI}$
BC6	7.00	3.11	2.25
B6	5.45	3.08	1.77
BC7	10.33	3.35	3.08
B7	6.75	3.03	2.22
BC8	7.90	3.63	2.17
B8	7.01	2.89	2.42
average value			2.31

Table 8 Experimental and theoretical cracked moment of inertia

beam no.	$I_{cr(th)} \times 10^6/mm^4$	$I_{cr(exp)} \times 10^6/mm^4$
BC6	452.98	385.84
B6	378.61	243.41
BC7	506.02	420.53
B7	453.73	326.00
BC8	513.79	421.29
B8	467.50	388.37

1) As it was expected by adding compressive reinforcement to singly reinforced HSC beams, the depth of natural axis at yield and ultimate state is decreased.

2) Experimental ultimate strength of specimens give reasonable estimation with what would be predicted by following the ACI 318-11 and CSA-04 codes provisions to use classic analytical equations. The average ratios of experimental strength to predicted strength were 0.994 and 1.002 for ACI 318-11 and CSA-04 code provisions, respectively. Therefore the strength of HSC heavily steel reinforced beam were quite close to that of the predicted by codes recommends.

3) As mentioned an important and challenging design issue for HSC reinforced beams is the serviceability requirement of deflection, and the two important parameters values that are influenced are cracking moment, M_{cr}, and cracked moment of inertia, I_{cr}. It can be found that the theoretical cracking moment and cracking moment of inertia are greater than experimental cracking moment. Therefore, the expressions which have been recommended for M_{cr} and I_{cr} in code provisions do not estimate a reasonable prediction for such parameters values. The ACI 318-11 code provisions are found to underestimate the maximum deflection of HSC reinforced beams at service load. A reasonable estimate can be made by considering an age-adjusted modulus of elasticity and premature cracking of the beams due to shrinkage and associated creep of concrete. The cracking moment of HSC reinforced beam is predicted by ACI 318-11 and CSA-04 codes without the considerations for shrinkage-induced stresses and the associated creep. The effects of which seem to be indirectly accounted for by using a conservative expression for modulus of rupture.

Nomenclature

X_u	neutral axis at ultimate state
M_u	ultimate moment carried by the section
φ_u	ultimate curvature at midspan
φ_y	curvature at yielding of tension reinforcement at midspan
α	the stress block coefficient
β	the ratio between the height of the stress block and X_u
E_s	modulus of elasticity of steel reinforcement
ρ	tension reinforcement ratio ($\rho = A_s/bd$)
ρ'	compression reinforcement ratio ($\rho' = A'_s/bd$)
f_y	yielding stress in tension reinforcement
f'_s	stress in compressive reinforcement
b	width of beam section
d	effective depth
d'	the distance compression reinforcement to top surface of beam
f'_c	compressive strain of concrete
l	clear span of beam
n	modular ratio($n = E_s/E_c$)
M_a	maximum bending moment in the span
M_{cr}	cracking moment
a	shear span
c	neutral axis depth from the top surface of the beam
f_r	the modulus of rupture of concrete
I_{cr}	moment of inertia of cracked transformed section
I_e	effective moment of inertia
I_{exp}	experimental moment of inertia
I_g	moment of inertia of gross concrete section ignoring reinforcement
A_s	area of tension longitudinal
A'_s	area of compression longitudinal
E_c	modulus of elasticity of concrete
M_y	yield moment
Δ_u	experimental ultimate deflection at midspan
ε_{cu}	experimental ultimate strain in compressive concrete at midspan
ε_{su}	experimental ultimate strain in tension reinforcement at midspan
ε_{cy}	the measured compression strain in the concrete at yielding of steel reinforcement
ε_{sy}	the measured tensile strain in steel reinforcement at yielding stage
w_c	concrete density

References

1. Maghsoudi A A, Sharifi Y. The serviceability considerations of HSC heavily steel reinforced members under bending. American Journal of Applied Sciences, 2008, 5(9): 1135–1140
2. Maghsoudi A A, Sharifi Y. Ductility of high strength concrete heavily steel reinforced members. Scientia Iranica Journal, 2009, 16 (4): 297–307
3. Hashemi S H, Maghsoudi A A, Rahgozar R. Bending response of HSC beams strengthened with FRP sheets. Scientia Iranica Journal, 2009, 16(2): 138–14
4. Lopes S M R, Bernardo L F A. Plastic rotation capacity of high-strength concrete beams. Materials and Structures, 2003, 36: 22–31
5. ACI Committee 318. Building code requirements for structural concrete (ACI 318–11) and commentary. Farmington Hills, MI:

American Concrete Institute, 2011
6. Ashour S A, Wafa F F. Flexural behavior of high strength fiber reinforced concrete beams. ACI Structural Journal, 1993, 90(3): 279–287
7. Wafa F F, Ashour S A. Mechanical properties of high-strength fiber reinforced concrete. ACI Materials Journal, 1992, 89(5): 449–455
8. Nilson A H. Design implication of current research on high strength concrete, High-Strength Concrete. ACI SP-87, American Concrete Institute, Detroit, 1987, 85–109
9. Ahmad S H, Barker R. Flexural behavior of reinforced high strength light concrete beams. ACI Materials Journal, 1991, 88(1): 69–77
10. Ashour S A. Effect of compressive strength and tensile reinforcement ratio flexural behavior of high-strength concrete beams. Engineering Structures, 2000, 22(5): 413–423
11. Ashour S A, Wafa F F, Kamal M I. Effect of the concrete compressive strength and tensile reinforcement ratio on the flexural behavior of fibrous concrete beams. Engineering Structures, 2000, 9 (22): 1133–1146
12. Khuntia M, Ghosh S K. Flexural stiffness of reinforced concrete columns and beams. ACI Structural Journal, 2004, 101(3): 351–363
13. Lambotte H, Taerwe L R. Deflection and cracking of high strength concrete beams and slabs, high-strength concrete. In: Hester W T, e d. Proceedings of the 2nd International Symposium. SP-121, American Concrete Institute, Farmington Hills, Mich, USA, 1990, 109–128
14. Leslie K E, Rajagopalan K S, Everard N J. Flexural behavior of high-strength concrete beams. ACI Structural Journal, 1976, 73(9): 517–521
15. Lin C H, Ling F S, Hwang C L. Flexural behavior of high-strength fly ash concrete beams. Journal of the Chinese Institute of Engineers, 1992, 15(1): 85–92
16. Mansur M A, Chin M S, Wee T H. Flexural behavior of high-strength concrete beams. ACI Structural Journal, 1997, 94(6): 663–674
17. Ozbakkaloglu T, Saatcioglu M. Rectangular stress block for high-strength concrete. ACI Structural Journal, 2004, 101(4): 475–483
18. Paster J A, Nilson A H, Slate F O. Behavior of High-strength Concrete Beams. Report No. 84–3, Department of Structural Engineering, Cornell University, USA, 1984
19. Paulson K A, Nilson A H, Hover K C. Long-term deflection of high-strength concrete beams. ACI Materials Journal, 1991, 88(2): 197–206
20. Pendyala R, Mendis P, Patnaikuni I. Full-range behavior of high-strength concrete flexural members comparison of ductility parameters of high and normal-strength concrete members. ACI Structural Journal, 1996, 93(1): 30–35
21. Sarker S, Adwan O, Munday J G L. High strength concrete: an investigation of the flexural behavior of high strength RC beams. Structural Engineer, 1997, 75(7): 115–121
22. Tognon G, Ursella P, Coppetti G. Design and properties of concretes with strength over 1500 kgf/cm^2. ACI Journal Proceedings, 1980, 77(3): 171–178
23. Swamy R N. High strength concrete–material properties and structural behavior high-strength concrete. ACI SP-87, American Concrete Institute, Detroit, 1987, 110–146
24. Rashid M A, Mansur M A. Reinforced high-strength concrete beams in flexural. ACI Structural Journal, 2005, 102(3): 462–471
25. CSA Technical Committee. Canadian Standards Association. CAN3–A23.3–M04, Rexdale, Ontario, Canada, 2004
26. Sharifi Y. Effect of tensile and compressive over reinforcement ratio on ductility and behavior of high-strength concrete flexural members. Master Thesis, Kerman: University of Kerman, 2005
27. Mohammad Hasani M. Ductility of reinforcement high-strength concrete beams with high longitudinal tensile reinforcement ratio (Special for Seismic Areas)". Master Thesis, Kerman: University of Kerman, 2004
28. MacGregor J, Wight J K. Reinforced concrete mechanics and design: Fourth edition in SI units. Upper Saddle River, NJ: Prentice Hall, 2006
29. Ghali A. Deflection of reinforced concrete members, A Critical Review. ACI Structural Journal, 1993, 90(4): 364–373
30. ACI 363R–10. Report on High-Strength Concrete, 2010, 65